


## RESEARCH ARTICLE

WILEY

# C5 conserved region of hydrophilic C-terminal part of *Saccharomyces cerevisiae* Nha1 antiporter determines its requirement of Erv14 COPII cargo receptor for plasma-membrane targeting

Klara Papouskova <sup>1</sup> | Michaela Moravcova<sup>1</sup> | Gal Masrati<sup>2</sup> | Nir Ben-Tal<sup>2</sup> | Hana Sychrova<sup>1</sup> | Olga Zimmermannova<sup>1</sup>

<sup>1</sup>Laboratory of Membrane Transport, Institute of Physiology of the Czech Academy of Sciences, Prague 4, Czech Republic

<sup>2</sup>Department of Biochemistry and Molecular Biology, George S. Wise Faculty of Life Sciences, Tel-Aviv University, Tel-Aviv, Israel

## Correspondence

Klara Papouskova, Laboratory of Membrane Transport, Institute of Physiology of the Czech Academy of Sciences, Videnska 1083, 14220 Prague 4, Czech Republic.  
Email klara.papouskova@fgu.cas.cz

## Funding information

USA-Israel Binational Science Foundation, Grant/Award Number: 2017293; Czech Science Foundation, Grant/Award Number: 17-01953S; Abraham E. Kazan Chair in Structural Biology, Tel Aviv University; Edmond J. Safra Center for Bioinformatics fellowship, Tel-Aviv University

## Abstract

Erv14, a conserved cargo receptor of COPII vesicles, helps the proper trafficking of many but not all transporters to the yeast plasma membrane, for example, three out of five alkali-metal-cation transporters in *Saccharomyces cerevisiae*. Among them, the Nha1 cation/proton antiporter, which participates in cell cation and pH homeostasis, is a large membrane protein (985 aa) possessing a long hydrophilic C-terminus (552 aa) containing six conserved regions (C1–C6) with unknown function. A short Nha1 version, lacking almost the entire C-terminus, still binds to Erv14 but does not need it to be targeted to the plasma membrane. Comparing the localization and function of ScNha1 variants shortened at its C-terminus in cells with or without Erv14 reveals that only ScNha1 versions possessing the complete C5 region are dependent on Erv14. In addition, our broad evolutionary conservation analysis of fungal Na<sup>+</sup>/H<sup>+</sup> antiporters identified new conserved regions in their C-termini, and our experiments newly show C5 and other, so far unknown, regions of the C-terminus, to be involved in the functionality and substrate specificity of ScNha1. Taken together, our results reveal that also relatively small hydrophilic parts of some yeast membrane proteins underlie their need to interact with the Erv14 cargo receptor.

## KEYWORDS

alkali-metal-cation homeostasis, cargo receptor, COPII, Erv14, Nha1, yeast

## 1 | INTRODUCTION

Intracellular homeostasis needs to be tightly regulated in all living cells, including the model yeast *Saccharomyces cerevisiae*. Various transport systems localized either in the plasma membrane or in the membranes of organelles cooperate to ensure the proper concentrations of alkali metal cations in cellular compartments (reviewed in (Arino *et al.*, 2010)).

The Nha1 Na<sup>+</sup>, K<sup>+</sup>/H<sup>+</sup> antiporter (Prior *et al.*, 1996) belonging to the CPA1 group of cation/proton antiporters (CPAs, (Masrati

*et al.*, 2018)) resides in the plasma membrane of yeast cells, where it is involved in the export of alkali metal cations using the energy of the electrochemical gradient of protons generated by the Pma1 H<sup>+</sup>-ATPase. Thanks to its broad substrate specificity for four alkali metal cations (Li<sup>+</sup>, Na<sup>+</sup>, K<sup>+</sup>, and Rb<sup>+</sup>), it not only takes part in the detoxification of cells, but also plays a housekeeping role while being involved in the maintenance of cell potassium homeostasis, intracellular pH, or plasma-membrane potential (Prior *et al.*, 1996; Banuelos *et al.*, 1998; Kinclova *et al.*, 2001b; Kinclova-Zimmermannova *et al.*, 2006). Nha1 is a large polytopic

transmembrane protein which is predicted to be composed of a short hydrophilic N-terminus, at least 12 transmembrane domains connected by short loops, and a cytoplasmically oriented long hydrophilic C-terminal part (552 of a total of 985 amino-acid residues) (Kinclova-Zimmermannova *et al.*, 2015). Previously, comparisons of Nha homologs from various yeast species revealed a very high level of sequence conservation in the transmembrane domains and connecting loops (Pribylova *et al.*, 2006), and also six conserved regions (C1–C6), whose function is not known, located in their hydrophilic C-terminal parts (Kamauchi *et al.*, 2002). With the exception of the C1 region located just behind the last transmembrane segment, the C-terminal part of Nha1 is dispensable both for its cation-antiporter function and localization in the plasma membrane. However, the C-terminus plays an important role in the regulation of Nha1 activity, both positively and negatively (Kinclova *et al.*, 2001b; Kamauchi *et al.*, 2002). The C-terminal part of Nha1 also participates in the regulation of the cell cycle and in the cell response to osmotic shock, which is connected to the phosphorylation of the Nha1 C-terminus by the kinase Hog1 (Simon *et al.*, 2001; 2003; Proft and Struhl, 2004; Kinclova-Zimmermannova and Sychrova, 2006). Recently, we showed the interaction of the C-terminal part of Nha1 with regulatory 14-3-3 proteins, resulting in a negative regulation of Nha1 (Zahradka *et al.*, 2012; Smidova *et al.*, 2019).

To perform their physiological functions, all transporters must be properly targeted to the site of their function in the plasma membrane or in the membranes of particular organelles. *S. cerevisiae* Erv14 is a member of the cornichon family of proteins conserved in fungi, plants, and also animals (Roth *et al.*, 1995; Castro *et al.*, 2007; Rosas-Santiago *et al.*, 2015). Erv14 is a cargo receptor of COPII vesicles that ensure the transport of proteins from the ER to the Golgi apparatus (Powers and Barlowe, 1998; 2002). It is a 14-kDa integral membrane protein with three predicted transmembrane domains. It helps to incorporate its cargoes into COPII vesicles by the simultaneous binding of both the cargo and Sec24, a COPII complex subunit. In the absence of Erv14, its cargoes are at least partially stacked in the ER of cells. The PAIRS (pairing analysis of cargo receptors) approach showed that Erv14 is required for the ER exit of approximately one third of the plasma-membrane proteins tested (18 of 57) (Herzig *et al.*, 2012). So far, about 40 diverse cargoes of Erv14 have been identified; mainly transporters (including some cation transporters (Herzig *et al.*, 2012; Rosas-Santiago *et al.*, 2016; Zimmermannova *et al.*, 2019)), and proteins involved in budding, sporulation, cell wall synthesis, and other processes (Powers and Barlowe, 1998; Nakanishi *et al.*, 2007; Sacristan *et al.*, 2013). With at least some Erv14 cargoes, its function may be partially substituted by Erv15, a paralog of the Erv14 protein (Powers and Barlowe, 1998; Pagant *et al.*, 2015).

The interactions of Erv14 with its cargoes and COPII vesicles are not yet fully understood. So far, several amino-acid residues of the Erv14 molecule have been shown to be critical for its function. Amino acids 97–101 (IFRTL) from the cytoplasmic loop of Erv14 have been identified to be necessary for the interaction of Erv14 with

the COPII coat (Powers and Barlowe, 2002), and also mutations of the luminal DYPE site (amino acids D<sub>33</sub>, Y<sub>34</sub>, P<sub>50</sub>, and E<sub>51</sub>) reduce the incorporation of Erv14 into ER-derived vesicles (Pagant *et al.*, 2015). The FLN site (F<sub>62</sub>, L<sub>63</sub>, and N<sub>74</sub>) located in the second transmembrane domain of Erv14 seems to be part of a binding site of some, but not all, Erv14 cargo proteins (Pagant *et al.*, 2015). A C-terminal acidic motif of Erv14, which is shared by fungi and plant cornichons, also participates in the interaction with at least three different plasma-membrane transporters (Rosas-Santiago *et al.*, 2017).

Despite differing significantly in their structure and function, all known Erv14 cargoes are membrane-spanning proteins working in the plasma membrane or late secretory pathway. A comparison of membrane proteins with a single transmembrane domain from both fungi and vertebrates showed a difference in the length of transmembrane domains between the early and late parts of the secretory pathway, with longer transmembrane domains in proteins in the trans-Golgi network, endosomes, and plasma membrane (Sharpe *et al.*, 2010). As no specific Erv14-binding motif has been identified in its cargoes, it was suggested that Erv14 recognizes its cargo proteins based on their structure, namely the length of their transmembrane domains (Herzig *et al.*, 2012). This proposal was experimentally confirmed by shortening a synthetic poly-leucine transmembrane domain that replaced the native transmembrane segment of Mid2, a cargo protein of Erv14, in increments of two amino-acid residues, given a set of variants with transmembrane domains in the range of 14–26 residues. Only the trafficking of variants with longer transmembrane domains was dependent on the presence of Erv14 (Herzig *et al.*, 2012).

The role of Erv14/cornichon proteins in the proper trafficking of some ion transporters seems to be conserved in various and phylogenetically distant groups of organisms. Mammalian Erv14 homologs, CNIH2 and CNIH3, are involved in the trafficking and also regulation of gating of ionotropic AMPA-type glutamate receptors (Schwenk *et al.*, 2009). In plants, the rice cornichon OsCNIH was found to interact with the Golgi-localized sodium transporter OsHKT1;3 (Rosas-Santiago *et al.*, 2015). Moreover, in *Arabidopsis thaliana*, CNIH proteins play a role in the sorting and activation of pollen-expressed glutamate receptor-like Ca<sup>2+</sup> channels (Wudick *et al.*, 2018). Studying the role of yeast Erv14 in the maintenance of alkali-metal-cation homeostasis, we recently showed that this COPII cargo receptor is important for the maintenance of several physiological parameters, such as cell size, plasma-membrane potential, and intracellular pH (Zimmermannova *et al.*, 2019). Moreover, the lack of Erv14 affects the growth of cells in the presence of low potassium levels or in media supplemented with high concentrations of toxic sodium or surplus potassium (Rosas-Santiago *et al.*, 2016; Zimmermannova *et al.*, 2019). These phenotypes result from the fact that we have identified three out of five plasma-membrane transporters mediating the fluxes of alkali metal cations as Erv14 cargoes—the Na<sup>+</sup>, K<sup>+</sup>/H<sup>+</sup> antiporter Nha1, the K<sup>+</sup> importer Trk1, and K<sup>+</sup> channel Tok1 (Rosas-Santiago *et al.*, 2016; Zimmermannova *et al.*, 2019). The reason of the lack of interaction of Erv14 with other two plasma-membrane

alkali-metal-cation transporters, Ena1 and Trk2, is not known at this moment, but may be connected to various factors, such as different expression patterns, transporters' structure, or interaction with other specific cargo receptors (discussed in (Zimmermannova *et al.*, 2019)).

As for Nha1, we have shown that it physically interacts with Erv14 via its transmembrane segments (Rosas-Santiago *et al.*, 2016). However, no intracellular stacking was observed for the C-terminally shortened Nha1 in *erv14Δ* cells (Nha1 long 472 aa, lacking the majority of its C-terminal part), despite the fact that this truncated protein may still bind the Erv14 protein (Rosas-Santiago *et al.*, 2016). This finding points to the specific requirements of Nha1 with its long C-terminus in the transporter's exit from the ER.

The aim of this work was to study the putative role of the presence, of specific amino-acid region(s) and/or size of the large hydrophilic C-terminal portion of Nha1 in the transporter's requirement of Erv14 for efficient transport through the secretory pathway. To achieve this, we used two different approaches: (i) the heterologous expression of yeast Nha1 homologs differing in the lengths of their C-termini and (ii) the production of various C-terminally shortened versions of ScNha1. The localization and function of all these proteins were compared in pairs of *S. cerevisiae* strains differing in the presence or absence of Erv14. Taken together, our results show that the presence of the C5 C-terminal conserved region of ScNha1 determines the transporter's requirement of Erv14 for its transport through the secretory pathway. In addition, we identified new specific regions of the ScNha1 C-terminus that are important for the antiporter's proper localization and determination of its substrate specificity and cation-extrusion efficiency at the whole-cell level.

## 2 | RESULTS

### 2.1 | Lack of Erv14 affects the proper localization of some heterologous yeast Nha antiporters in *S. cerevisiae* cells

Full-length Nha1 (985 aa long) requires the help of Erv14 to be properly transported through the secretory pathway and localized in the plasma membrane of cells. This requirement of Erv14 disappears

when Nha1 lacks the majority of its hydrophilic C-terminal part (i.e., is shortened by 513 aa), despite the fact that the shortened Nha1 version (Nha1-472) is still able to bind Erv14 (Rosas-Santiago *et al.*, 2016). As the C-terminal part of Nha1 forms 56% of the whole molecule, we wanted to determine whether it is the presence of a specific region of the C-terminus or the large size of this hydrophilic part of the transporter which determines the antiporter's requirement of Erv14.

For this purpose, we used the BW31 strain (a salt-sensitive derivative of W303-1A lacking its own Nha1 and Ena Na<sup>+</sup>, K<sup>+</sup> ATPases, Table 1), because this strain was previously used to study the effect of C-terminal shortening on the function of Nha1 (Kinclova *et al.*, 2001b) and to characterize all Nha1 homologs used in this study (see below). As the effect of *ERV14* deletion on the salt tolerance of *S. cerevisiae* cells has so far been only shown in the BY4741 genetic background (Rosas-Santiago *et al.*, 2016), we first deleted the *ERV14* gene in both the W303-1A and BW31 strains, and verified whether *ERV14* deletion also results in a salt sensitivity as in the BY4741 background. As Figure S1 shows, W303-1A *erv14Δ* cells grew slightly worse in the presence of both 1,500 mM NaCl and 1,800 mM KCl than cells possessing Erv14. An even higher impact of the lack of Erv14 on the salt tolerance of cells was observed in the salt-sensitive BW31 strain (Figure S1). Thus generally, the effect of *ERV14* deletion on salt tolerance is similar in both W303-1A and BY4741 strains and their salt-sensitive derivatives lacking alkali-metal-cation exporters.

As an initial approach, we heterologously expressed eight Nha1 homologs from various yeast species in BW31 cells with or without Erv14. All the studied antiporters were previously functionally expressed in BW31 cells (Kinclova *et al.*, 2001a; Papouskova and Sychrova, 2006; Velkova and Sychrova, 2006; Krauke and Sychrova, 2008; 2011; Pribylova *et al.*, 2008). Figure 1a shows the phylogenetic relatedness of these Nha proteins and the differing lengths of their C-termini, which range from only 93 amino acids in YINha2 to 562 amino-acid residues in ZrNha1 (Figure 1a, numbers in parentheses, Table S1).

All heterologous Nha proteins were properly targeted to the plasma membrane of BW31 cells (Figure 1b). The shortest antiporter, YINha2, was not only observed in the plasma membrane, but also in the ER, which might be the result of the synthesis of more copies of this short protein within a cell cycle. The lack of Erv14 did

Strain	Genotype	Source/References
W303-1A	<i>MATa leu2-3/112 ura3-1 trp1-1 his3-11/15 ade2-1 can1-100</i>	(Wallis <i>et al.</i> , 1989)
W303-1A <i>erv14Δ</i>	W303-1A <i>erv14Δ::loxP</i>	This work
BW31	W303-1A <i>ena1Δ::HIS3::ena4Δ nha1Δ::LEU2</i>	(Kinclova-Zimmermannova <i>et al.</i> , 2005)
BW31 <i>erv14Δ</i>	BW31 <i>erv14Δ::loxP</i>	This work
BYT45	BY4741 <i>nha1Δ::loxP ena1-5Δ::loxP</i>	(Navarrete <i>et al.</i> , 2010)
BYT45 <i>erv14Δ</i>	BYT45 <i>erv14Δ::loxP</i>	(Rosas-Santiago <i>et al.</i> , 2016)

TABLE 1 Strains used in this study

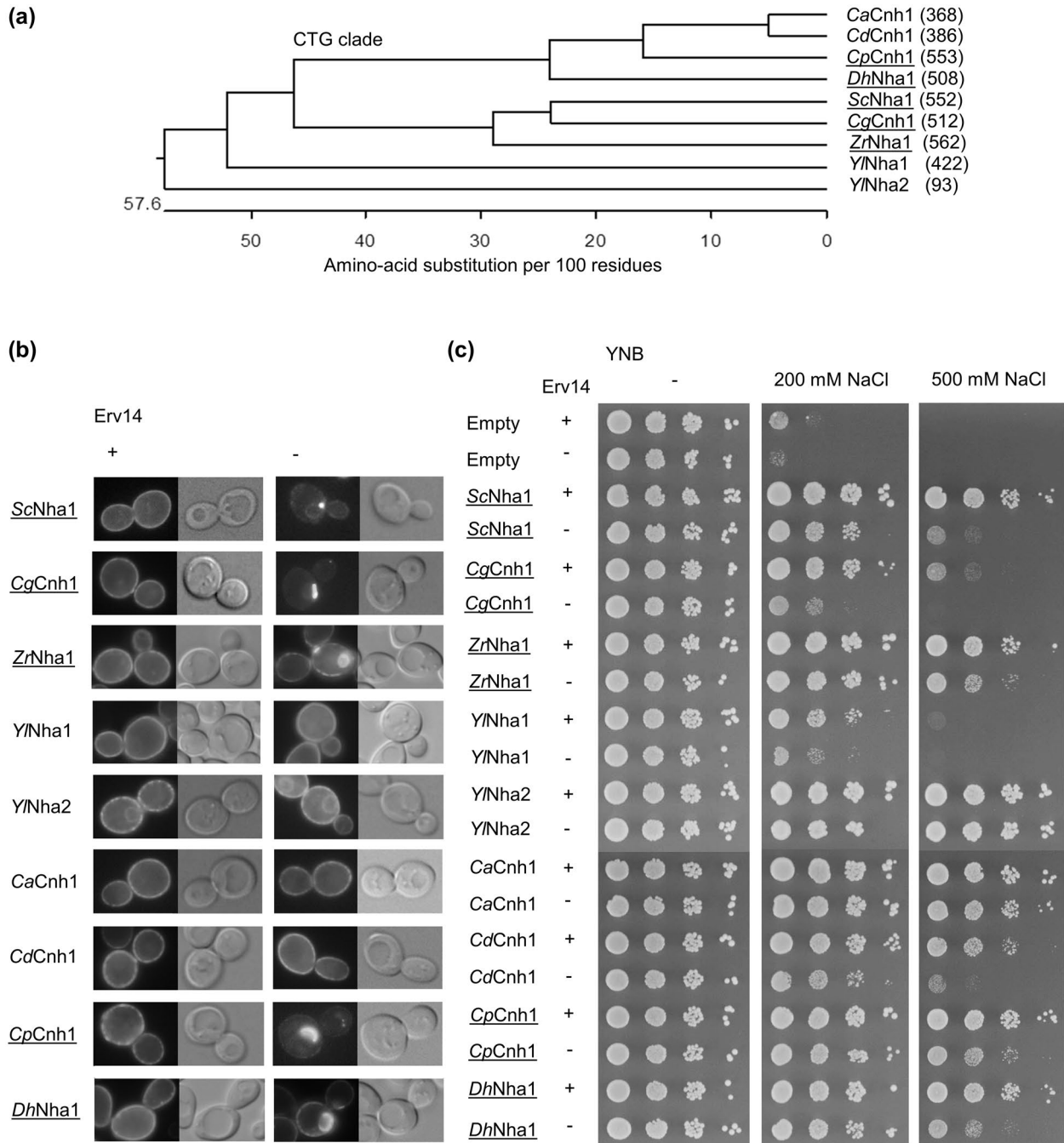


**FIGURE 1** Localization and function of various yeast Nha antiporters in *Saccharomyces cerevisiae* BW31 and BW31erv14Δ cells. (a) Phylogenetic tree of studied yeast Nha antiporters. Numbers in parentheses show the length in amino acids of their C-termini. (b) Fluorescence (left) and Nomarski (right) pictures of BW31 cells with or without Erv14 producing various yeast Nha antiporters tagged with GFP. (c) NaCl tolerance of BW31 cells with or without Erv14, containing an empty vector (pGRU1) or producing various yeast GFP-tagged Nha antiporters, determined on YNB plates supplemented as indicated. Pictures were taken after 3 days of growth at 30°C. *Ca*, *Candida albicans*, *Cd*, *C. dubliniensis*, *Cg*, *C. glabrata*, *Cp*, *C. parapsilosis*, *Dh*, *Debaryomyces hansenii*, *Sc*, *S. cerevisiae*, *Yl*, *Yarrowia lipolytica*, and *Zr*, *Zygosaccharomyces rouxii*. Erv14-dependent antiporters are underlined

not affect the localization of CaCnh1, CdCnh1, and both Y/Nha antiporters, as we did not observe differences in the GFP signal between BW31 and BW31erv14Δ cells producing these antiporters (Figure 1b). In contrast, besides the expected ScNha1, we observed a partial intracellular antiporter stacking in BW31erv14Δ cells producing CgCnh1, ZrNha1, CpCnh1, and DhNha1 (Figure 1b). We also

observed similar results in the BY4741 genetic background (strains BYT45 and BYT45erv14Δ, not shown).

Even in the absence of Erv14, all Nha1 homologs were at least partially functional in the plasma membrane of BW31 cells, as their presence increased the tolerance of cells to sodium compared to the growth of cells transformed with an empty vector (Figure 1c).

Cells producing individual antiporters but lacking *Erv14* grew worse in the presence of toxic sodium cations in comparison to cells with functional *Erv14* and antiporters. For *Y1Nha2*, which actively extrudes sodium from cells (Papouskova and Sychrova, 2006), this effect of the absence of *Erv14* was observed in the presence of NaCl concentrations higher than 1 M (not shown). A direct comparison of the effect of *ERV14* deletion on the salt tolerance of cells producing individual *Nha1* homologs was impeded due to the already lower sodium tolerance of *BW31erv14Δ* versus *BW31* cells (Figures S1, 1c 200 mM NaCl, cells with empty vector) as well as by the significantly differing sodium export abilities of the studied antiporters. Nevertheless, the consequence of *erv14Δ*-dependent mislocalization could be clearly observed for example, for *CaCnh1* and *CpCnh1*. These two efficient sodium exporters (Krauke and Sychrova, 2008) that enabled *BW31* cells to grow similarly well in the presence of 500 mM NaCl, differed in their provision of sodium tolerance to *erv14Δ* cells (Figure 1c) in agreement with the fact that only the plasma-membrane localization of *CpCnh1* was affected in cells lacking *Erv14* (Figure 1b).

Looking at the relatedness of the studied *Nha* antiporters (Figure 1a), *ERV14* deletion affected the localization of antiporters phylogenetically close to *ScNha1* (*CgCnh1* and *ZrNha1*) and two transporters from yeasts belonging to the CTG clade (*CpCnh1* and *DhNha1*). The plasma-membrane localization of *Cnh1* antiporters from *C. albicans* and *C. dubliniensis* and two *Nha* antiporters from the phylogenetically distant *Y. lipolytica* was not affected in *erv14Δ* cells. Interestingly, *ERV14* deletion only affected the trafficking of *Nha1* homologs with long (more than 500 amino-acid residues) hydrophilic C-terminal parts (Figure 1a, Table S1). In summary, our results suggested that the *Nha* antiporters' requirement of *Erv14* is (i) either conserved in some yeast species in relation to their phylogenetical relatedness, or (ii) is determined by the length of the C-terminal hydrophilic part of the antiporter.

## 2.2 | C-terminal shortening by about 190 amino-acid residues results in the loss of the *Nha1* requirement of *Erv14*

To further reveal either the critical length or to specify the region of *ScNha1* C-terminus responsible for the antiporter's *Erv14* requirement, we determined the localization and function of *Nha1* versions with gradually shortened C-termini in *BW31* cells lacking or possessing *Erv14*. At first, we tested six shortened versions of *Nha1*. Figure 2 shows the topological model of *Nha1* (Kinclova-Zimmermannova *et al.*, 2015) with highlighted conserved regions C1–C6 (Kamauchi *et al.*, 2002) present in its C-terminus and sites of C-terminal shortenings (designated according to the lengths of the resulting *Nha1* versions in amino-acid residues). The previously studied full-length *Nha1*-985 (*Erv14*-dependent) and the shortest *Nha1*-472 (*Erv14*-independent) were used as controls.

As shown in Figure 3a, the lack of *Erv14* affected, besides *Nha1*-985, the proper plasma-membrane localization of the two longest shortened versions of *Nha1* (*Nha1*-928 and -858). These proteins were partially stacked inside *erv14Δ* cells and the peripheral GFP signal was much weaker than in *BW31* cells producing these *Nha1* versions (Figure 3a). On the other hand, *ERV14* deletion did not alter the localization of *Nha1*-799 and shorter versions. For some of these versions (*Nha1*-740, -680, and -472) we observed a GFP signal not only in the periphery of cells, but also in the perinuclear ER, irrespective of the presence or absence of *Erv14*. An unusual "patchy" pattern of GFP signal was observed together with the cell periphery and perinuclear ER in cells producing *Nha1*-799 (Figure 3a), which is shortened inside the C5 conserved region (Figure 2), suggesting that this version of *Nha1* is at least partially mislocalized, even in *BW31* cells with functional *Erv14* (Figure 3a). A not fully homogeneous peripheral GFP signal was also observed in *BW31* cells producing *Nha1*-858 (Figure 3a).

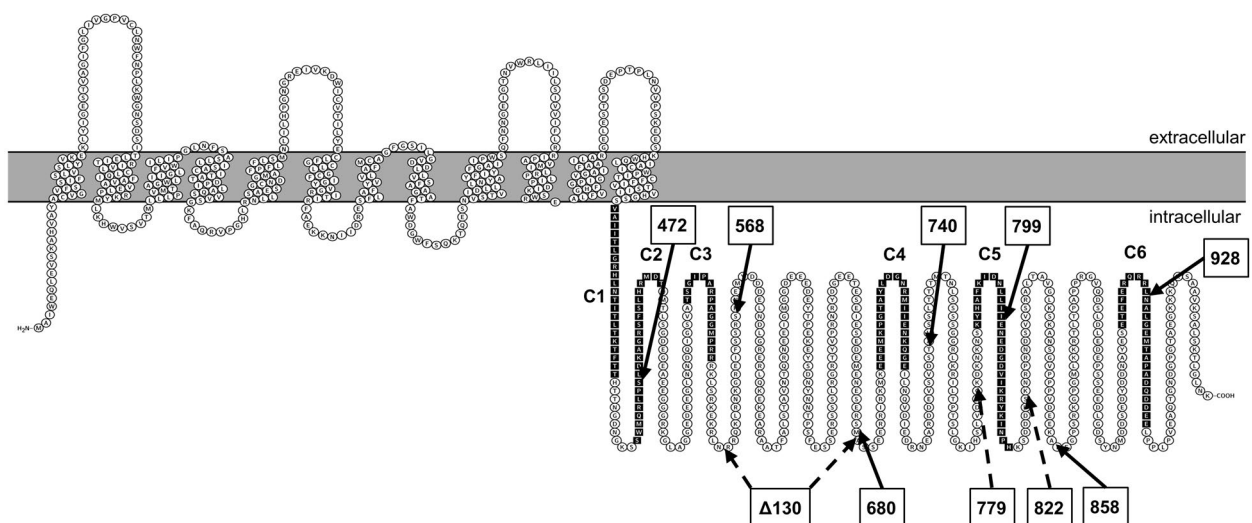


**FIGURE 2** Topological model of *S. cerevisiae* *Nha1* with sites of shortenings of studied *Nha1* versions with their lengths indicated by the numbers in boxes. Full arrows—first set of C-terminal shortenings, dashed arrows—second set of C-terminal shortenings.  $\Delta 130$ —arrows show the starting and end points of the internal C-terminal deletion. Amino-acid residues forming C-terminal conserved regions C1–C6 are shown in black

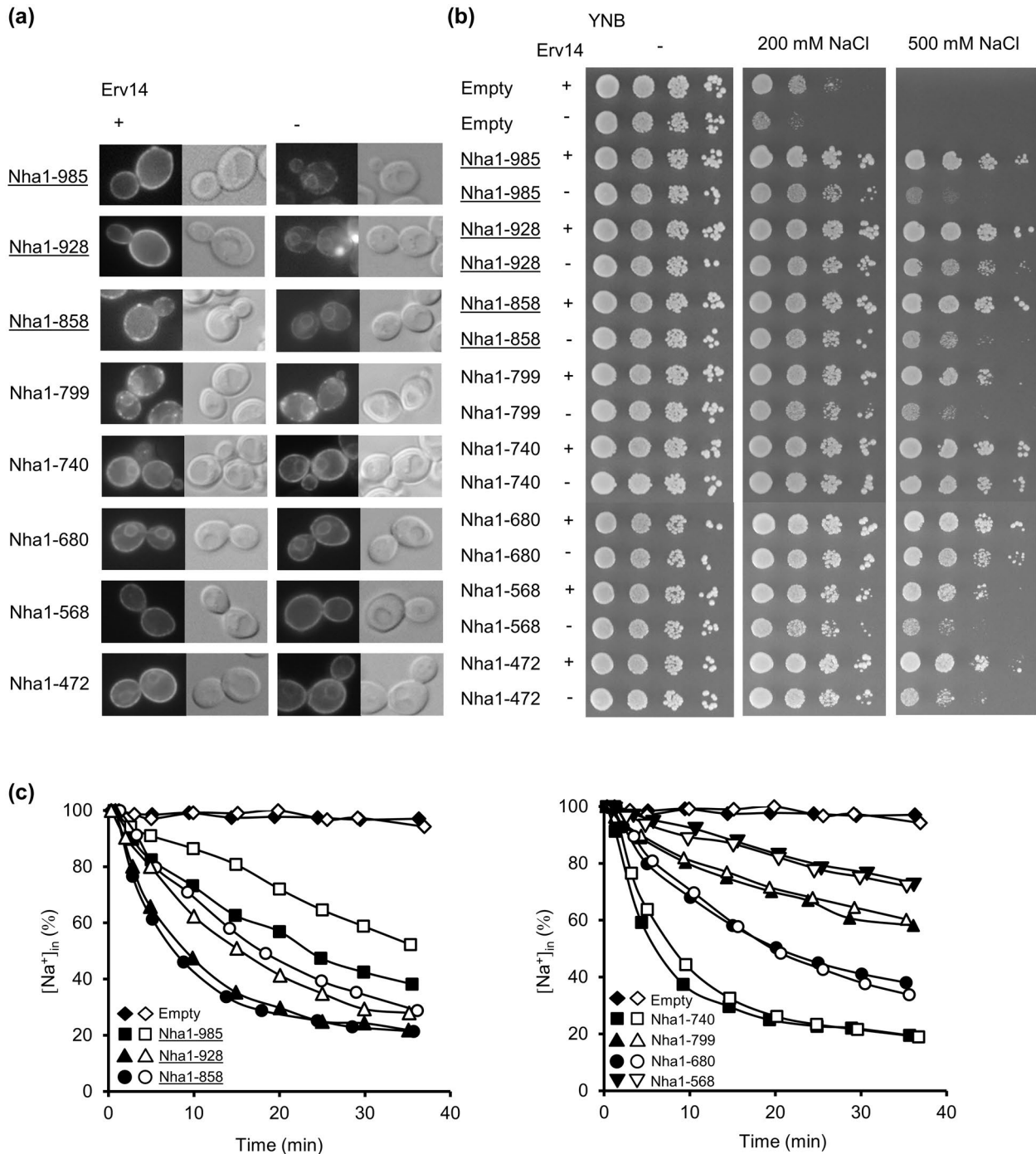


**FIGURE 3** Localization and function of *S. cerevisiae* Nha1 and its C-terminally shortened versions in BW31 and BW31erv14Δ cells. (a) Fluorescence (left) and Nomarski (right) pictures of BW31 cells with or without Erv14 producing full-length Nha1 (Nha1-985) or its C-terminally shortened versions tagged with GFP. (b) NaCl tolerance of BW31 cells with or without Erv14 containing an empty vector (YEp352) or producing full-length Nha1 or its C-terminally shortened versions determined on YNB plates supplemented as indicated. Pictures were taken after 3 days of growth at 30°C. (c) Sodium efflux from BW31 (full symbols) or BW31erv14Δ (empty symbols) cells containing empty vector (YEp352), or producing full-length Nha1 or its C-terminally shortened versions. Cells were grown in YNB media, preloaded with NaCl and Na<sup>+</sup> loss was estimated as described in Experimental procedures. Data are from one typical experiment. Erv14-dependent versions are underlined

The C-terminal GFP tagging of the antiporters did not change the sodium tolerance of cells producing particular Nha1 versions (Figure S2). Nevertheless, to study the effect of C-terminus length on Nha1 functioning in more detail, we used YEp352-based plasmids

without the GFP tag to avoid the potential influence of prolonging the C-terminus by 238 amino acid long GFP. When comparing the functionality, that is, the ability to increase cell tolerance to salts, all Nha1 versions were able to increase the sodium tolerance of

BW31 and BW31*erv14Δ* cells, although the effectivity of individual versions varied (Figure 3b) in accord with the previously published finding that the shortening of the Nha1 C-terminus influences the export activity of Nha1, especially for toxic sodium and lithium cations (Kinclova *et al.*, 2001b). A slight shortening of Nha1 to 928, 858, and 740 amino acids, respectively, resulted in a moderately better growth of BW31 cells producing these Nha1 versions in the presence of NaCl in comparison with the growth of cells with the full-length protein (500 mM NaCl, compare the size of colonies in the final dilution). This observation is in agreement with the autoinhibitory role of the very terminal portion of the antiporter's C-terminus (Kinclova *et al.*, 2001b). The Nha1-799 version provided BW31 cells with a lower sodium tolerance than both longer (Nha1-858) and shorter (Nha1-740) versions, most likely as a result of the observed partial mislocalization of this particular Nha1 version (Figure 3a). The sodium tolerance of BW31 cells producing Nha1-680 was similar to the NaCl tolerance of cells producing Nha1-985, while the shorter versions, Nha1-568 and Nha1-472, were less efficient than the full-length Nha1 (Figure 3b), which is again in agreement with previous results (Kinclova *et al.*, 2001b). The observed sodium tolerance differences among cells producing particular Nha1 versions were confirmed in Na<sup>+</sup> efflux measurements (see, below and Figure 3c).

The lack of Erv14 diminished the salt tolerance of cells producing individual Nha1 versions to various extents (Figure 3b). Versions whose localization was apparently less affected by the absence of Erv14 provided the cells with an accordingly less affected salt tolerance (e.g., Nha1-740 and Nha1-680, Figure 3a,b). Nevertheless, the observed worse growth of all *erv14Δ* cells in the presence of NaCl might be the result of either the mislocalization of particular antiporters, the lower general sodium tolerance of the BW31*erv14Δ* strain compared to BW31 (Figures S1 and 3b 200 mM NaCl, cells with empty vector), or a combination of both factors. Thus, to determine the direct effect of *ERV14* deletion on the sodium extrusion efficiency of cells producing particular Nha1 versions, we compared

Na<sup>+</sup> efflux mediated by Nha1 versions in cells with or without Erv14 (Figure 3c).

After sodium preloading (see, Experimental procedures), the cells contained a sufficient initial amount of Na<sup>+</sup> (140 ± 31 nmol/mg dry weight in average), and its efflux could be followed effectively (Figure 3c). As no Na<sup>+</sup> loss was observed in cells lacking cation exporters (cells transformed with an empty vector), the decrease in Na<sup>+</sup> content in cells producing individual Nha1 versions was exclusively the result of the functioning of the antiporter present (Figure 3c).

Similarly to the phenotype of salt tolerance in drop tests, the ability of individual Nha1 versions to mediate sodium efflux varied. The Nha1-740, -858, and -928 versions provided BW31 cells with a better ability to export Na<sup>+</sup> than the full-length protein (Nha1-985, Figures 3c and 4 full bars, Table S2). Sodium export from BW31 cells producing Nha1-680 was similar to the export measured from cells with the full-length Nha1. On the other hand, sodium loss from cells with the Nha1-799 and -568 versions was significantly lower (Figures 3c and 4 full bars, Table S2); in cells with Nha1-799, the decrease in sodium efflux was probably a consequence of the observed partial mislocalization of this Nha1 version in BW31 cells (Figure 3a).

The partial intracellular stacking of native Nha1 (Nha1-985) resulted in a lower sodium efflux from *erv14Δ* cells compared to cells with functional Erv14 (Figures 3c left panel, 4 compare full and empty bars), in agreement with previous results (Rosas-Santiago *et al.*, 2016). Similarly, and as expected from our microscopic observations and the drop tests, *ERV14* deletion resulted in a significantly lower sodium export from cells producing the Nha1-928 and -858 versions (Figures 3c left panel, 4, Table S2), but it did not affect the sodium loss from cells with shorter versions, whose localization was not changed in cells lacking the Erv14 protein (Figures 3c right panel, 4, Table S2). Thus we showed that the partial intracellular stacking of the long Nha1 versions resulted in a lower sodium efflux from *erv14Δ* cells.

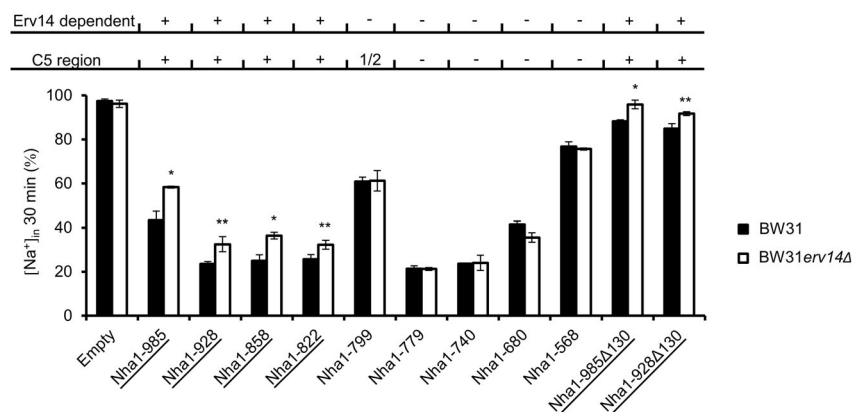


**FIGURE 4** Sodium content in BW31 (full bars) and BW31*erv14Δ* (empty bars) cells producing *S. cerevisiae* Nha1 or its C-terminally shortened versions after a 30min incubation in a Na<sup>+</sup>-free buffer. [Na<sup>+</sup>]<sub>in</sub> in the beginning of measurement corresponds to 100%. Data are means ± standard deviation. Asterisks denote significantly higher values in BW31*erv14Δ* cells than in BW31 cells producing the same Nha1 version (\**p* < 0.05, \*\**p* < 0.01). The presence/absence (±) of the C5 region and Erv14 dependence of the antiporters are indicated. 1/2—approx. half of the C5 is present. Erv14-dependent versions are underlined

In summary, the comparison of the localization of shortened Nha1 versions and the sodium-export efficiency of cells harboring them showed that the Nha1 versions truncated by 186 or more amino acids (Nha1-799 and shorter versions) are not dependent on the presence of Erv14. Importantly, all Erv14-dependent Nha1 versions were shortened behind the C5 C-terminal conserved region (Figure 2).

### 2.3 | The presence of the C5 C-terminal conserved region determines the Nha1 requirement of Erv14

To further elucidate whether the loss of Erv14 requirement of Nha1 version -799 and shorter is connected solely to the reduced lengths of these antiporter versions or with the loss/disruption of the C5 C-terminal region, we prepared four additional Nha1

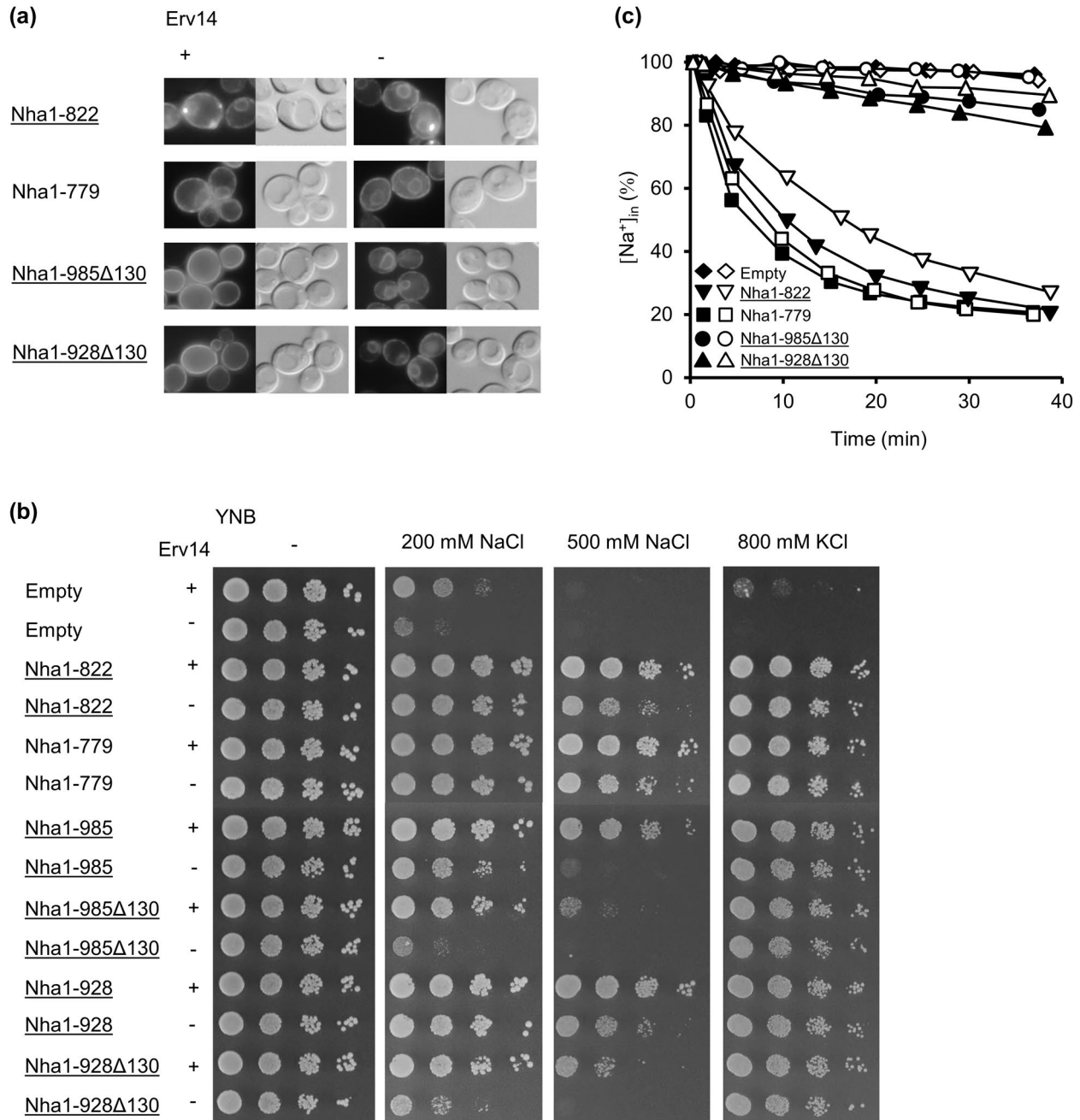


**FIGURE 5** Localization and function of *S. cerevisiae* Nha1-822, -779, and  $\Delta 130$  versions in BW31 and BW31erv14 $\Delta$  cells. (a) Fluorescence (left) and Nomarski (right) pictures of BW31 cells with or without Erv14 producing C-terminally shortened Nha1 versions tagged with GFP. (b) NaCl and KCl tolerance of BW31 cells with or without Erv14 containing an empty vector (YEp352) or producing full-length Nha1 or its C-terminally shortened versions was determined on YNB plates supplemented as indicated. Pictures were taken after 3 days of growth at 30°C. (c) Sodium efflux from BW31 (full symbols) or BW31erv14 $\Delta$  (empty symbols) cells containing empty vector (YEp352), or producing Nha1 C-terminally shortened versions. Cells were grown in YNB media, preloaded with NaCl and Na<sup>+</sup> loss was estimated as described in Experimental procedures. Data are from one typical experiment. Erv14-dependent versions are underlined



versions and the localization and function of them were again determined in BW31 cells in the presence or absence of *Erv14*. First, we shortened *Nha1* to lengths of 822 and 779 amino-acid residues (Figure 2). These versions allowed us to specify the length/region responsible for the *Erv14* requirement in more detail without disrupting the C5 region, which strongly affected both the localization and export efficiency of the antiporter (*Nha1-799* version, Figure 3).

The *Nha1-822* version, shortened closely (7 aa) behind the C5 region (Figure 2), was localized both to the periphery and perinuclear ER in both types of cells (Figure 5a). Similarly to what we observed for *Nha1-858*, and more strongly for *Nha1-799* in cells with *Erv14* (Figure 3a), the localization of *Nha1-822* was not fully homogenous, with patches of a stronger signal in some cells (Figure 5a). *Nha1-779*, shortened closely (7 aa) before the C5 (Figure 2), was detected both in the periphery and in the ER of both types of cells (Figure 5a) similarly to what we observed for the shorter *Nha1* versions -740 and -680 (Figure 3a). Both *Nha1-822* and -779 efficiently provided BW31 cells with sodium tolerance (Figure 5b). Nevertheless, the function of *Nha1-822* seemed to be more affected by the lack of *Erv14* than the function of the shorter *Nha1-779* antiporter (compare the growth of *erv14Δ* cells producing both antiporters in the presence of 500 mM NaCl; Figure 5b). The dependence of *Nha1-822* on *Erv14* was confirmed in sodium efflux measurements (Figures 4 and 5c, Table S2). In contrast, the lack of *Erv14* did not affect sodium export in cells producing *Nha1-779* (Figures 4 and 5c, Table S2). In summary, the *Nha1-822* version shortened closely behind the C5 region was still functionally dependent on the presence of *Erv14* according to  $\text{Na}^+$  efflux measurements, though we did not observe significant differences in the localization of *Nha1-822* in the presence or absence of *Erv14* (Figure 5). On the other hand, the *Nha1-779*, ending just before the C5 region, was independent of *Erv14*.

Second, we internally shortened the C-termini of the *Nha1-985* and -928 versions by deleting 130 amino-acid residues from the less conserved amino-acid stretch between the C3 and C4 C-terminal regions (Figure 2). These  $\Delta 130$  *Nha1* versions contained all C1-C6 conserved C-terminal regions with the exception of the second half of C6 in *Nha1-928Δ130* (the C6 region does not influence the *Nha1* requirement of *Erv14*, as *Nha1-858* lacking the C6 is *Erv14*-dependent, Figure 3). Moreover, both  $\Delta 130$  versions have both the C5 region and its surroundings fully preserved. The C-terminal lengths of the *Nha1-985Δ130* or -928 $\Delta 130$  versions corresponded to the lengths of the above studied shortest *Erv14*-dependent (*Nha1-858*) or longest *Erv14*-independent (*Nha1-799*) antiporter versions, respectively (Table S1).

Both the *Nha1-985Δ130* and -928 $\Delta 130$  antiporters were exclusively localized in the plasma membrane of BW31 cells, showing that the  $\Delta 130$  deletion did not affect the antiporter's plasma-membrane targeting (Figure 5a). On the other hand, both  $\Delta 130$  versions were observed not only in the periphery but also in the perinuclear ER of cells without *Erv14*, suggesting that both these shortened antiporters require *Erv14* for their trafficking via the secretory pathway (Figure 5a).

Surprisingly, the deletion of 130 amino-acid residues between the C3 and C4 conserved regions strongly affected the antiporter's ability to support the growth of BW31 cells in the presence of sodium (Figure 5b), suggesting that the region between the C3 and C4 is important for the full transport efficiency of *Nha1*, though it does not belong among the six known conserved regions of the yeast *Nha* antiporters. BW31 cells producing *Nha1-928Δ130* grew better in the presence of NaCl than cells with *Nha1-985Δ130* (Figure 5b), showing that the effect of  $\Delta 130$  deletion is independent of the effect of the lack of the very C-terminal autoinhibitory part of *Nha1* (Kinclova *et al.*, 2001b). The sodium tolerance of *erv14Δ* cells producing  $\Delta 130$  *Nha1* versions was lower than the tolerance of the corresponding BW31 cells, similarly to what we observed for all studied *Nha* antiporters (Figure 5b). The less efficient *Nha1-985Δ130* version was not able to increase the sodium tolerance of *erv14Δ* cells compared to cells transformed with the empty vector, though a proportion of its molecules seemed to be localized to the plasma membrane (Figure 5a). To see if this version is functional in *erv14Δ* cells, we tested the growth of cells in the presence of 800 mM KCl, a concentration which strongly inhibits the growth of BW31*erv14Δ* cells lacking cation exporters (Figures S1 and 5b cells with empty vector). Under these conditions, *Nha1-985Δ130* was able to support the growth of *erv14Δ* cells similarly to all other tested *Nha1* versions, showing that it did not lose its ability to export cations completely (Figure 5b). Measurements of sodium export from cells with or without *Erv14* confirmed that the  $\Delta 130$  deletion highly affected the ability of *Nha1-985* and -928 to export sodium from BW31 cells. The lack of *Erv14* resulted in an even lower sodium efflux with *Nha1-928Δ130*, and no sodium efflux was observed in BW31*erv14Δ* cells producing *Nha1-985Δ130* (Figures 4 and 5c, Table S2).

Figure 4 and Table S2 give a summary of all of our  $\text{Na}^+$  efflux measurements, and clearly show that the C-terminal shortening of *Nha1* leading to the disruption or deletion of the C5 region results in the loss of the antiporter's *Erv14* requirement. The partial intracellular stacking in cells without *Erv14* and the *Erv14*-dependence of the *Nha1-928Δ130* version, whose C-terminus is as short as in a version which does not require *Erv14* (*Nha1-799*), showed us that it is not solely the length of the C-terminal part of the antiporter, but more importantly the presence of the C5 conserved region which determines the *Nha1* requirement of *Erv14*.

## 2.4 | *Nha1-779* and -740 are efficient cation exporters whose production affects the growth of cells in the presence of low $\text{K}^+$

Our drop test experiments and sodium efflux measurements (Figures 3–5, Table S2) showed that the C-terminal shortenings of *Nha1* inside and in the surroundings of the C5 C-terminal region influence the functioning of the antiporter. To further examine in detail the importance of this region or other specific C-terminal regions for *Nha1* transport properties and physiological functions, we tested the growth of BW31 cells producing individual *Nha1*

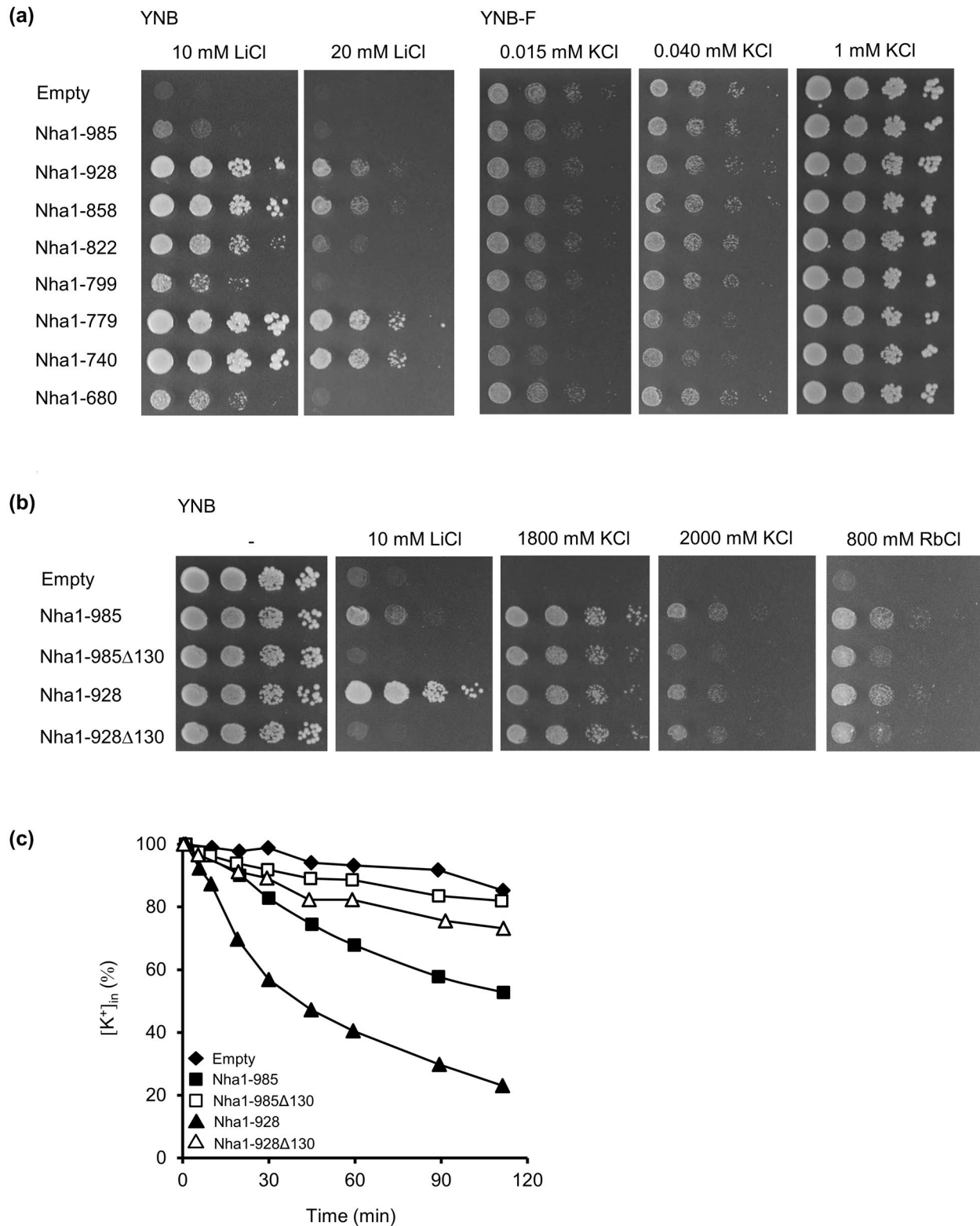


**FIGURE 6** Salt tolerance and potassium-efflux efficiency of BW31 cells producing various *S. cerevisiae* Nha1 versions. (a) LiCl and low-KCl tolerance of BW31 cells containing an empty vector (YEp352) or producing full-length Nha1 or its C-terminally shortened versions. (b) LiCl, KCl, and RbCl tolerance of BW31 cells containing an empty vector (YEp352) or producing Nha1-985, -928, and corresponding  $\Delta 130$  versions. Growth was determined on YNB or YNB-F plates supplemented as indicated. Pictures were taken after 4 or 5 (RbCl) days of growth at 30°C. (c) Potassium efflux from BW31 cells containing empty vector (YEp352), or producing full-length Nha1 or its C-terminally shortened versions. Cells were grown in YNB media and  $K^+$  loss was estimated as described in Experimental procedures. Initial potassium amount in cells was  $441 \pm 37$  nmol/mg dry weight. Data are from one typical experiment

versions in the presence of highly toxic lithium cations, another substrate of Nha1 antiporters. The full version of Nha1 (Nha1-985) is only able to slightly increase the tolerance of BW31 cells to lithium (Figure 6a, (Kinclova *et al.*, 2001b)). The shortening of the very end of the Nha1 C-terminus results in a higher lithium export activity of Nha1 (Kinclova *et al.*, 2001b), leading to a higher  $\text{Li}^+$  tolerance of cells producing the Nha1-928 and -858 versions in comparison with cells producing the full-length antiporter (Figure 6a, Table S2). The shortening of Nha1 closely behind (Nha1-822) and inside (Nha1-799) the C5 region resulted in a decrease in Nha1's ability to support the growth of cells in the presence of lithium as a result of the partial mislocalization (more pronounced in Nha1-799) of these two Nha1 versions in BW31 cells (Figures 3, 5, and 6a, Table S2). Interestingly, when the complete C5 region was discarded (Nha1-779 and -740 versions), the ability of Nha1 to provide BW31 cells with lithium tolerance was highly enhanced, suggesting an increased capacity of these two versions to export lithium. Further C-terminal shortening at position 680 resulted in a decrease in the lithium tolerance of cells (Figure 6a).

The potentially increased transport efficiency of Nha1-779 and Nha1-740, visible in sodium efflux capacity (Figure 4) and lithium tolerance (Figure 6a), was verified in growth tests of cells producing Nha1 variants under conditions of limited potassium. Yeast cells need to accumulate high intracellular concentrations of potassium (approx. 200–300 mM) to support growth and provide the turgor necessary for cell division (Arino *et al.*, 2010). Nha1, thanks to its ability to export  $\text{K}^+$ , contributes to the maintenance of cell potassium homeostasis, that is, participates in the necessary continuous uptake and efflux of potassium, which regulate cell plasma-membrane potential and thereby other physiological parameters such as intracellular pH (Zahradka and Sychrova, 2012). When  $\text{K}^+$  is scarce in the environment, an increased potassium export might be detrimental for cells, as they would have to cope with a higher  $\text{K}^+$  loss and spend more energy to accumulate the necessary amount of potassium. Our growth tests on plates with low-potassium YNB-F medium showed that while all the tested Nha1 versions supported a similar growth of cells in the presence of 1 mM KCl, the production of the Nha1-779 and -740 antiporters decreased the ability of cells to grow on plates with 15 and 40  $\mu\text{M}$  KCl (Figure 6a). This result confirmed that despite their partial ER localization (Figures 3 and 5) the Nha1-779 and Nha1-740 versions provide cells with higher ion-extrusion efficiency than the others.

## 2.5 | Amino-acid residues between the C3 and C4 C-terminal conserved regions are important for Nha1's ability to export alkali metal cations

The deletion of 130 amino-acid residues between Nha1 C-terminal conserved regions C3 and C4 (Figure 2) resulted in a significant decrease in the antiporter's ability to export sodium (Figures 4 and 5, Table S2), without an apparent defect in the plasma-membrane localization of Nha1 (Figure 5a). To see whether the  $\Delta 130$  deletion

only affects the ability of Nha1 to export sodium, or other alkali metal cations as well, we compared the lithium, high potassium, and rubidium tolerance of BW31 cells producing Nha1-985 $\Delta 130$  and Nha1-928 $\Delta 130$ . As Figure 6b shows, the  $\Delta 130$  deletion completely abolished the ability of Nha1 to improve cell lithium tolerance, even with the Nha1-928 version which enables a better growth of cells in the presence of LiCl than the full-length protein (Figure 6b, Table S2). On the other hand, tolerance to high concentrations of potassium seemed to be slightly decreased only with Nha1-985 $\Delta 130$  and both  $\Delta 130$  versions were able to support the growth of cells in the presence of the fourth Nha1 substrate, rubidium, although less efficiently than corresponding Nha1 versions without the internal deletion (Figure 6b). As we have shown previously, the ability of Nha antiporters to support the long-term growth in the presence of high amounts of nontoxic potassium not always fully corresponds to the rate of potassium efflux from cells; even a low  $\text{K}^+$  loss measured in the absence of extracellular surplus of potassium can be sufficient to ensure the growth of cells on plates (Kinclova-Zimmermannova *et al.*, 2005; Papouskova and Sychrova, 2006). Thus to examine the impact of the  $\Delta 130$  deletion on the antiporter's ability to extrude  $\text{K}^+$ , we compared potassium efflux from BW31 cells producing Nha1-985, -928, and corresponding  $\Delta 130$  versions. As Figure 6c clearly shows, potassium loss from cells producing the  $\Delta 130$  versions was much lower than  $\text{K}^+$  efflux from cells with Nha1-985 or the very efficient -928 version, similarly to what we observed with sodium (Figures 4 and 5, Table S2).

Taken together, our results show that the deletion of 130 amino acids between the C3 and C4 regions significantly lowers the Nha1 antiporter's efficiency in alkali-metal-cation extrusion at the whole-cell level and especially affects the ability of Nha1 to support the growth of cells in the presence of the smallest Nha1 substrate, highly toxic lithium.

## 2.6 | Evolutionary conservation analysis reveals new conserved regions in C-terminal parts of fungal Nha1 homologs

Our experiments with various C-terminally shortened versions of ScNha1 provided new information about the importance of several regions of the Nha1 C-terminus for the antiporter's proper trafficking, localization and cation-extrusion efficiency. To obtain more knowledge about putative structural and functional elements in the C-terminal parts of yeast Nha antiporters, we extended a previous sequence comparison of Nha1 homologs (Kamauchi *et al.*, 2002) and performed a broad evolutionary conservation analysis of C-termini in fungal Nha1 homologs.

A multiple sequence alignment consisting of 286 sequences from the entire kingdom of fungi (see Experimental procedures for sequence search and clustering) was used in a ConSurf (Ashkenazy *et al.*, 2016) analysis (Figure S3) with ScNha1 as the reference sequence. Figure S4 depicts 25 sequences that were sampled from the larger multiple sequence alignment, including ScNha1 and its yeast

homologs used in this study (Figure 1). Purple boxes mark positions that ranked above the confidence cut-off with a conservation grade that is equal or higher than 6 on the ConSurf conservation scale (1 being the most variable and 9 the most conserved).

Originally, six conserved regions C1–C6 were identified in the C-terminal parts of Nha antiporters, based on a comparison of sequences from six yeast species and *Aspergillus nidulans* (Kamauchi *et al.*, 2002). Using a much larger data set of fungal Nha antiporters, we were able to confirm the presence of the C1 to C6 regions in the C-termini of yeast Nha proteins, but we also identified new evolutionarily conserved regions (Figure S4) in yeast Nha1 homologs. These new amino-acid segments either extend the previously described C1–C6 regions, allowing us to determine their boundaries more precisely, or represent newly found conserved regions (Figure S4). We found the C1–C4 regions to be only slightly (1–5 amino-acid residues) longer than previously predicted, and we identified two new and highly charged evolutionarily conserved regions located between the C3 and C4 regions.

For the C5 region, the newly found conserved extension is much longer than its originally determined length (approx. 46 vs. 30 amino-acid residues; Figures S4 and 7). In the close vicinity of C5, we found one short conserved segment preceding it, and another conserved segment localized shortly behind its end (Figures S4 and 7), which could mean that in fact it is a single relatively long conserved region. All these findings confirm the importance of the C5 region and its surroundings.

### 3 | DISCUSSION

The synthesis of plasma-membrane transporters begins in the endoplasmic reticulum, from which they are sorted to the Golgi apparatus via COPII vesicles. *S. cerevisiae* Nha1 was identified as a binding partner of Erv14, which serves as a cargo receptor in COPII vesicles (Herzig *et al.*, 2012; Rosas-Santiago *et al.*, 2016). The functional independence of a version of Nha1 which lacks the majority of its

long hydrophilic C-terminal part (Nha1-472 version) on Erv14 (Rosas-Santiago *et al.*, 2016) suggested that the Nha1 C-terminus plays a role in the antiporter's trafficking. This work identifies the C5 C-terminal conserved region to be responsible for Nha1's requirement of Erv14 for proper plasma-membrane targeting and consequent functioning. In addition, we provide new information about the role of specific regions of the large hydrophilic C-terminal portion of Nha1 in its proper localization and cation-export efficiency.

Recently, we have shown that the interaction of Erv14 with the Trk1 K<sup>+</sup> importer in *S. cerevisiae* seems to be conserved in other yeast species, as Trk1 homologs from *C. glabrata* and *C. albicans* were mislocalized upon heterologous expression in *S. cerevisiae* *erv14Δ* cells (Zimmermann *et al.*, 2019). Our pilot experiments, in which we produced various yeast Nha homologs in *S. cerevisiae* cells in the presence or absence of Erv14 (Figure 1), suggested a phylogenetically conserved interaction of Erv14 with Nha antiporters at least in yeasts related to *S. cerevisiae* (*C. glabrata* and *Z. rouxii*) and some species belonging to the CTG clade (*C. parapsilosis* and *D. hansenii*).

Only the trafficking of heterologous antiporters that possessed a long hydrophilic C-terminus (longer than 500 amino acids, Figure 1) was affected by the absence of Erv14, which corresponded well with our previous observation that ScNha1 with a short C-terminus does not need Erv14 for its targeting to the plasma membrane (Rosas-Santiago *et al.*, 2016). In order to reveal whether it is really only the length or a specific region of the ScNha1 C-terminal part which determines the antiporter's requirement of Erv14, we studied the localization and function of a series of C-terminally shortened versions of ScNha1 in cells with or without Erv14. This approach led us to the conclusion that the shortening of about 190 amino-acid residues at the very end of the C-terminus results in the loss of the antiporter's requirement of the Erv14 cargo receptor for its plasma-membrane targeting (Figure 3). Nevertheless, the finding that all Erv14-dependent ScNha1 versions also possessed a complete C5 C-terminal region (Figures 3–5, Table S2), together with the observed Erv14 dependence of the Nha1-928Δ130 antiporter (Figures 4 and 5, Table S2), which is relatively short but contains the intact C5

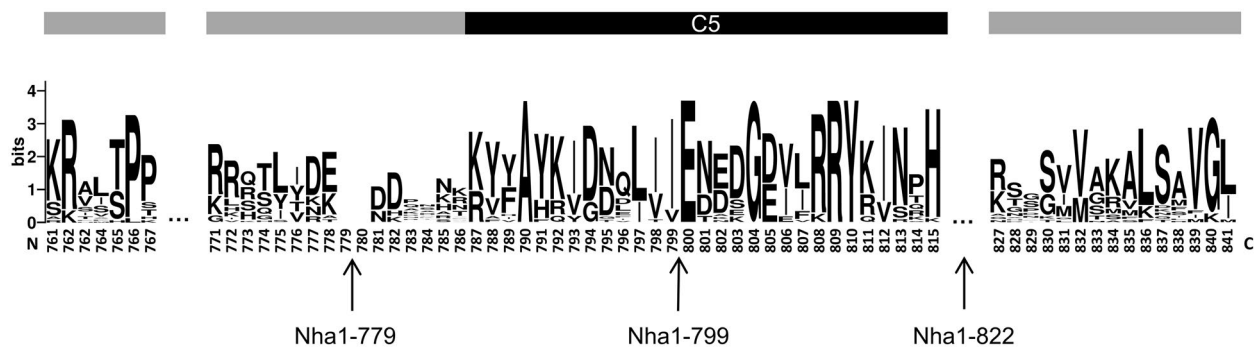


**FIGURE 7** Amino-acid patterns of the C5 C-terminal region (black box) and its surroundings. WebLogo analysis was based on yeast sequences (from organisms belonging to the order *Saccharomycetales*) shown in Figure S3. The overall height of a stack indicates the sequence conservation at a particular position, while the height of symbols within a stack indicates the relative frequency of each amino acid at that position. Numbers correspond to amino-acid positions in the C-terminus of ScNha1. Newly identified evolutionarily conserved regions are indicated with gray boxes. The arrows show positions of ScNha1 C-terminal shortenings. The ... mean that less conserved amino-acid stretches between individual conserved regions are not shown

region, showed unambiguously that it is not the length of the Nha1 C-terminal part that determines the antiporter's Erv14 requirement. In *S. cerevisiae*, the presence of the C5 region is the prerequisite of its Nha1 antiporter's need for the Erv14 cargo receptor to be efficiently transported via the secretory pathway.

On the other hand, and quite interestingly, the C5 region is conserved in most studied Nha1 homologs (Figure S4), including the *CaCnh1* and *CdCnh1* antiporters, whose plasma-membrane localization was not affected in *BW31erv14Δ* cells, though they are phylogenetically related to other antiporters that proved to be Erv14-dependent in *S. cerevisiae* cells (*CpCnh1* and *DhNha1*, Figure 1). More experiments would be needed to determine whether closely related *CaCnh1* and *CdCnh1* antiporters are at all binding partners of Erv14 (they possibly might have lost their ability to interact with Erv14 during their evolution), or determine the reason for their independence of *S. cerevisiae* Erv14 despite the presence of the C5 region in their C-termini. We cannot exclude the possibility that these antiporters efficiently interact with another cargo receptor of COPII vesicles in *C. albicans* and *C. dubliniensis* cells, or that observed small nuances in the primary structure of C5 regions (cf. Figure S4) could change the dependence of these two antiporters on ScErv14. Also, the secondary structure of particular C-termini might influence antiporters' trafficking from the ER. The distal part of the C-terminal tail of the human plasma-membrane  $\text{Na}^+/\text{H}^+$  exchanger NHE1 has been shown to be intrinsically disordered (Norholm *et al.*, 2011), and it was suggested that this part of protein contains conserved regions of a transient secondary structure. Such protein segments are believed to play a role in mediating protein-protein interactions (Vacic *et al.*, 2007). Mutation within such a molecular recognition feature results in an impaired exit of the NHE1 transporter from the ER (Norholm *et al.*, 2011), supporting the role of structural disorder in the trafficking of ion transport proteins. Interestingly, a high degree of structural disorder seems to be also typical for the *S. cerevisiae* Nha1 C-terminal part (Smidova *et al.*, 2019).

Further studies will be needed to elucidate how the C5 C-terminal region determines the ScNha1 requirement of Erv14. The transporter's exit from the ER seems to require not only proper folding, but also specific interactions with ER lipids, chaperones and also COPII-complex proteins (reviewed in (Diallinas and Martzoukou, 2019)). Proper oligomerization also seems to play a role in the packaging of membrane proteins into COPII vesicles and efficient trafficking via the secretory pathway (Springer *et al.*, 2014; Martzoukou *et al.*, 2015). Co-precipitation of differently tagged Nha1 proteins together with *in vitro* cross-linking experiments revealed that Nha1 forms dimers (Mitsui *et al.*, 2005). The dimerization seems to be important for the activity of the antiporter and may already occur in the ER membrane (Mitsui *et al.*, 2005). It was suggested that Erv14 plays a role in the dimerization of Nha1 (Rosas-Santiago *et al.*, 2016). The full-length antiporter can be detected as a dimer both in the plasma membrane and in the ER of cells with Erv14. On the other hand, Nha1-985 monomers were more abundant than the dimeric form in the ER, and no Nha1 dimers were detected in the plasma membrane in cells without Erv14 (Rosas-Santiago *et al.*, 2016). Moreover, no

apparent dimerization was detected with the shortened and Erv14-independent Nha1 version lacking the majority of its C-terminus (Nha1-472) (Rosas-Santiago *et al.*, 2016). Thus, the involvement of the C5 C-terminal region in Nha1 dimerization and consequently the antiporter's requirement of Erv14 is an interesting possibility, which we plan to address in the future.

Shortened versions of Nha1 lacking the C5 C-terminal region were efficiently transported to the plasma membrane irrespective of the presence or absence of Erv14. Whether they are transported from the ER to the Golgi apparatus solely by bulk flow in *erv14Δ* cells (Thor *et al.*, 2009; Barlowe and Miller, 2013) or if they are incorporated into COPII vesicles via their interaction with another COPII component still remains to be elucidated. Some Erv14 cargoes, such as the transporter Yor1, simultaneously bind Erv14 and Sec24 (Louie *et al.*, 2012; Pagant *et al.*, 2015), and the presence of Erv14 makes the trafficking of Yor1 more efficient (Pagant *et al.*, 2015). Another possibility is that an Erv14 homolog, Erv15 (Powers and Barlowe, 1998), might substitute for Erv14 when there are truncated versions of Nha1 in cells lacking Erv14. To date, there is no known specific cargo, whose transport from the ER to the Golgi apparatus is solely dependent on the presence of Erv15 (Herzig *et al.*, 2012), but Erv15 is able to partially substitute for the function of Erv14 (Pagant *et al.*, 2015).

The C5 region and the following amino-acid residues seem to play a role in proper Nha1 plasma-membrane targeting and consequently its cation-export efficiency, even in cells with functional Erv14. A negative effect of C-terminal shortening on the localization of Nha1 could be seemingly observed in the versions -858 and -822 (nonhomogeneous GFP signal, perinuclear ER stacking in case of Nha1-822, Figures 3a and 5a), but was most striking in Nha1-799 (Figure 3a). While Nha1-858 very efficiently supported the growth of *BW31* cells in the presence of both  $\text{Na}^+$  and  $\text{Li}^+$ , the sodium tolerance of cells producing Nha1-799 (shortened just in the middle of the C5 domain, Figures 2 and 7) was lower due to a less efficient sodium extrusion from cells with the -799 version, and both the -799 and -822 Nha1 versions provided cells with a lower lithium tolerance than Nha1-858 (Figures 3-6, Table S2). In contrast, shorter Nha1-779 and -740 versions (completely lacking the C5 region) exported sodium from cells and increased cell lithium tolerance very efficiently (Figures 3-6, Table S2). Thus the integrity of the C5 C-terminal region and the following amino-acid residues seems to be specifically important for proper Nha1 localization and functioning, although the presence of this region is not essential. Interestingly, the Nha1-799 version is shortened just before an ENEDGD sequence (Figures 2 and 7). D/E-X-D/E motifs (two acidic residues separated by any amino acid) were found to be involved in the ER exit of several viral, yeast, plant, and human proteins (Mikosch and Homann, 2009). Figures 7 and S4 show the phylogenetic conservation of these two putative Sec24-binding motifs in the C-termini of yeast Nha1 homologs. A new conserved amino-acid segment was identified closely behind the C5 region of yeast Nha proteins (Figures 7 and S4). This part of ScNha1 might also be important for the antiporter's proper plasma-membrane localization and functioning, as the Nha1-822

version, whose localization and also ability to provide cells with lithium tolerance were affected (Figures 5 and 6, Table S2), lacks this region.

Despite their partial ER localization in BW31 cells (Figures 3 and 5), Nha1-779 and -740 shortened before the C5 C-terminal region (Figure 2) were the most efficient versions used in this study. These antiporters efficiently supported the growth of cells in the presence of excess sodium, lithium and potassium cations (Figures 3, 5 and 6, Table S2) but their overproduction, resulting probably in an increased loss of potassium from cells, affected cell performance under conditions of low  $K^+$  levels in the environment (Figure 6). It is not known whether the presence of the C5 region might also play a role in an "autoinhibition" of the antiporter under conditions where the full activity of the transporter might be disastrous for cells. Alternatively, shortenings of Nha1 to the lengths of 779 or 740 amino acids, respectively, might change other protein's properties, for example, may improve its stability resulting in an increased cell ion-extrusion efficiency provided by these two particular Nha1 versions.

The proper plasma-membrane localization of the Nha1  $\Delta 130$  shortened versions together with their significantly lower ability to extrude sodium and potassium cations and as well as their inability to provide cells with lithium tolerance (Figures 4–6, Table S2) suggest that the relatively long stretch of amino acids located between the C3 and C4 regions participates in the determination of Nha1 cation-export efficiency and substrate specificity. The ConSurf analysis revealed new protein segments with a high degree of evolutionary conservation located between the C3 and C4 C-terminal regions (Figure S4). Nevertheless, despite a certain level of evolutionary conservation, these regions seem to differ even in various related groups of yeast species (e.g., yeasts related to *S. cerevisiae* or to *C. albicans*, Figure S4). We suggest that the  $\Delta 130$  deletion might have affected the proper conformation of the C-terminal part of Nha1, which resulted in the worse functioning of the antiporter and a complete loss of ability to support the tolerance of  $Li^+$  (Figure 6b). A similar modulation of the function/substrate specificity by cytosolic tails of transporters was shown for example, for the *A. nidulans* FurE, a uracil-allantoin-uric acid transporter (Papadaki *et al.*, 2017; 2019). Its N- and C-cytosolic tails interact with other internal loops of the transporter and thus regulate FurE fine gating and substrate specificity. Mutations within these regions can lead either to an extended number of substrates or to an increase in the transporter's specificity.

In conclusion, we show here, to the best of our knowledge for the first time, that a relatively small hydrophilic part of a plasma-membrane protein might be important for the protein's need for Erv14 COPII cargo receptor help. Until now, the length of transmembrane domains was the only known reason why the targeting of some membrane proteins was dependent on Erv14 (Herzig *et al.*, 2012). For the *S. cerevisiae* plasma-membrane Nha1 antiporter, we show that it is the C5 conserved region in its long hydrophilic C-terminus, which determines the requirement of Erv14.

In addition, our study revealed three very new and important results, not directly related to the function of Erv14. We found the C5 region and following amino-acid residues to play an important role

in proper Nha1 plasma-membrane localization and function, even in cells possessing Erv14. We also identified a stretch of amino acids located between the C3 and C4 regions as being very important for Nha1 proper functioning and substrate specificity. Finally, our new broad evolutionary conservation analysis of almost 300 fungal  $Na^+/H^+$  antiporters particularized the size and position of the already known six conserved C-terminal regions and revealed new conserved regions in the C-terminal hydrophilic parts of yeast Nha1 antiporters.

## 4 | EXPERIMENTAL PROCEDURES

### 4.1 | Yeast strains, media, growth conditions, and growth tests

The *S. cerevisiae* strains used in this study are listed in Table 1. The W303-1Aerv14 $\Delta$  and BW31erv14 $\Delta$  strains were prepared using homologous recombination and the Cre-loxP system (Guldener *et al.*, 1996) with the disruption cassettes and oligonucleotides listed in Table S3. BYT45 and the corresponding erv14 $\Delta$  strain are derivatives of *S. cerevisiae* BY4741 (MATa his3 $\Delta$ 1 leu2 $\Delta$ 0 met15 $\Delta$ 0 ura3 $\Delta$ 0, EUROSCARF). Yeast strains were grown at 30°C either in YPD (1% yeast extract, 2% peptone, 2% glucose) or in YNB (0.67% without amino acids, 2% glucose) media containing appropriate auxotrophic supplements. Two percentage agar was used for solid media. The growth of yeast strains on solid media in the presence of various concentrations of NaCl (100–1,500 mM), KCl (0.015–2,000 mM), LiCl (10–25 mM), or RbCl (800 mM) was monitored in drop test experiments. Ten-fold serial dilutions of fresh cell suspensions ( $OD_{600} = 2$ , Eppendorf BioPhotometer) were spotted on YNB or YNB-F (0.17% YNB-F without ammonium sulphate and potassium (ForMedium, (Navarrete *et al.*, 2010)), 0.4%  $(NH_4)_2SO_4$ , 2% glucose, pH adjusted to 5.8 with  $NH_4OH$ ) plates supplemented as indicated, and growth was monitored for 3–5 days. A representative result of three independent experiments with similar results is shown.

### 4.2 | Plasmids and plasmid construction

The plasmids used in this study are listed in Table S4. Genes encoding various Nha transporters were expressed from the same multicopy vectors (pGRU1, YEep352) under the control of the weak and constitutive ScNHA1 promoter. In pGRU1-based plasmids, a GFP-encoding sequence was added in frame to the 3' terminal part of the genes. New plasmids were prepared by homologous recombination in *S. cerevisiae* cells. The oligonucleotides used for DNA-fragment amplification are listed in Table S3. Amplified DNA fragments encoding C-terminally shortened versions of NHA1 were inserted into YEep352 or pGRU1 plasmids behind the NHA1 promoter, replacing the ENA1 gene in the plasmid pScENA1 or pScENA1-GFP (Zimmermannova *et al.*, 2019), respectively. The NHA1-985 $\Delta$ 130 and -928 $\Delta$ 130 versions were created from two separately amplified DNA fragments, one of them encoding Nha1 amino acids 1 to 551, and the second

fragment corresponding to the other part of Nha1-985 and -928, respectively, starting from amino acid 682. Both DNA fragments extended with homologous ends were then inserted into the YEp352 or pGRU1 plasmid by homologous recombination. *Escherichia coli* XL1-Blue (Stratagene) was used for plasmid amplification, and successful cloning was verified by restriction analysis and sequencing.

### 4.3 | Fluorescence microscopy

Microscopic pictures of exponentially growing cells ( $OD_{600} \approx 0.2-0.3$ , Spekol, Carl Zeiss) producing transporters C-terminally tagged with GFP were acquired using an Olympus BX53 microscope equipped with a Cool LED light source with 460 nm excitation and 515 nm emission and an Olympus camera DP73. Nomarski optics was used for whole-cell images.

### 4.4 | Cation loss determination

Sodium and potassium efflux were determined as previously described (Kinclova-Zimmermannova *et al.*, 2005). Briefly, cells were grown in YNB medium to the early exponential growth phase ( $OD_{600} \approx 0.2-0.3$ , Spekol, Carl Zeiss). To measure sodium loss, harvested cells were incubated in YNB supplemented with 100 mM NaCl at pH 7.0 (to preload them with sodium and to minimize the transport activity of Nha1, which is driven by the energy of the proton gradient across the plasma membrane) for 60 min. No preloading was necessary when potassium efflux was measured. Cells were collected by centrifugation, washed with deionised water, and resuspended in an incubation buffer containing 10 mM Tris, 0.1 mM  $MgCl_2$ , 2% glucose, and 10 mM KCl or 10 mM RbCl (to prevent  $Na^+$  or  $K^+$  reuptake, respectively), the pH was brought down to 4.4 with citric acid and adjusted to 4.5 with  $Ca(OH)_2$ . Aliquots of cells were withdrawn over a period of 40 (sodium loss) or 120 (potassium loss) min. Cells were harvested by filtration, washed with 20 mM  $MgCl_2$ , acid extracted, and the cation content was determined by atomic absorption spectrometry. Measurements were repeated with similar results, and data from one typical experiment (Figures 3, 5 and 6) or means  $\pm$  standard deviations (Figure 4, Table S2) are shown. Statistically significant differences were analyzed by an unpaired Student *t* test using MS Office Excel ( $*p < 0.05$ ,  $**p < 0.01$ ).

### 4.5 | Sequence analysis

The phylogenetic tree of Nha antiporters from various yeast species was produced using the software Lasergene from DNASTAR. The topology of Nha antiporters was predicted according to the model of ScNha1 (Kinclova-Zimmermannova *et al.*, 2015) based on a multiple sequence alignment (Lasergene, ClustalW algorithm). The Protter tool was used for ScNha1 secondary structure visualization (Omasits *et al.*, 2014).

### 4.5.1 | Evolutionary conservation analysis of C-terminal part of fungal Nha1 homologs

Plasma-membrane fungal CPAs were first retrieved from the manually curated Swiss-Prot database (Boutet *et al.*, 2016). This search yielded five sequences of yeast plasma-membrane Nha antiporters (UniProt entries Q99271, O42701, Q99173, O14123, and P36606). These sequences were then aligned using MAFFT (Katoh and Standley, 2013) with default parameters, and the alignment was utilized to produce an HMM profile using HMMER (Eddy, 1998). To broaden the sequence search, the HMM profile was then used in a HMMER search (e-value 0.0001) against the UniProt database (Apweiler *et al.*, 2004). This search resulted in a total of 2,767 fungal sequences. Fragmented sequences and sequences denoted with a "CAUTION" mark in UniProt were discarded, resulting in a "clean" data set of 1,264 sequences. Next, the sequences were clustered using CD-HIT (Huang *et al.*, 2010) with a 90% sequence identity threshold, resulting in 835 representatives.

In order to only retrieve the C-terminal part, a preliminary alignment was computed using MAFFT (Katoh and Standley, 2013) with default parameters. This alignment contained both the membrane and C-terminal regions. Next, the sequence of the archaeal CPA member NhaP1 from *Methanocaldococcus jannaschii* (MjNhaP1, UniProt entry Q60362) was introduced into the preliminary alignment. MjNhaP1 had its structure solved (Paulino *et al.*, 2014), and thus it was used to accurately discern between the membrane and C-terminal regions of the fungal antiporters. In addition, 20 random sequences were selected for an analysis using the transmembrane topology detector Phobius (Käll *et al.*, 2004). Both approaches placed the boundary between the membrane and C-terminal parts roughly in the same region. After discarding the membrane portion, we eliminated CPAs that lacked a significant C-terminus, by screening out all the sequences that contained more than 99% gaps. Finally, the remaining sequences were re-aligned and sequences that introduced large gaps into the alignment were discarded. The final multiple sequence alignment consisted of 286 sequences. The multiple sequence alignment was then used in a ConSurf (Ashkenazy *et al.*, 2016) analysis with the default settings. WebLogo (Schneider and Stephens, 1990; Crooks *et al.*, 2004) was used for graphical representations of amino-acid patterns of conserved regions in the C-termini of yeast Nha proteins.

### ACKNOWLEDGMENTS

This work was supported by grant 17-01953S from the Czech Science Foundation (OZ) and grant 2017293 of the USA-Israel Binational Science Foundation (NB-T). NB-T's research is supported in part by the Abraham E. Kazan Chair in Structural Biology, Tel Aviv University. GM was funded in part by a fellowship from the Edmond J. Safra Center for Bioinformatics at Tel-Aviv University.

### CONFLICT OF INTEREST

The authors declare no conflict of interest.

## AUTHOR CONTRIBUTIONS

Conceived and Designed Experiments: OZ, KP, and HS; Performed the experiments, Analyzed the Data: KP, MM, OZ, and GM; Drafted the Article: KP; Writing—review and editing: OZ, HS, GM, and NB-T; Prepared the Digital Images: KP and GM.

## DATA AVAILABILITY STATEMENT

The data that supports the findings of this study are available from the corresponding author upon a reasonable request.

## ORCID

Klara Papouškova  <https://orcid.org/0000-0002-1061-0940>

## REFERENCES

- Apweiler, R., Bairoch, A., Wu, C.H., Barker, W.C., Boeckmann, B., Ferro, S., et al. (2004) UniProt: the Universal Protein knowledgebase. *Nucleic Acids Research*, 32, D115–D119.
- Arino, J., Ramos, J. and Sychrova, H. (2010) Alkali metal cation transport and homeostasis in yeasts. *Microbiology and Molecular Biology Reviews*, 74, 95–120.
- Ashkenazy, H., Abadi, S., Martz, E., Chay, O., Mayrose, I., Pupko, T., et al. (2016) ConSurf 2016: an improved methodology to estimate and visualize evolutionary conservation in macromolecules. *Nucleic Acids Research*, 44, W344–W350.
- Banuelos, M.A., Sychrova, H., Bleykasten-Grosshans, C., Souciet, J.L. and Potier, S. (1998) The Nha1 antiporter of *Saccharomyces cerevisiae* mediates sodium and potassium efflux. *Microbiology*, 144, 2749–2758.
- Barlowe, C.K. and Miller, E.A. (2013) Secretory protein biogenesis and traffic in the early secretory pathway. *Genetics*, 193, 383–410.
- Boutet, E., Lieberherr, D., Tognolli, M., Schneider, M., Bansal, P., Bridge, A. J., et al. (2016) UniProtKB/Swiss-Prot, the manually annotated section of the UniProt knowledgebase: how to use the entry view. In: Edwards, D. (Eds.) *Plant Bioinformatics. Methods in Molecular Biology*, Vol. 1374. New York, NY: Humana Press. pp. 23–54.
- Castro, C.P., Piscopo, D., Nakagawa, T. and Derynck, R. (2007) Cornichon regulates transport and secretion of TGF $\alpha$ -related proteins in metazoan cells. *Journal of Cell Science*, 120, 2454–2466.
- Crooks, G.E., Hon, G., Chandonia, J.M. and Brenner, S.E. (2004) WebLogo: a sequence logo generator. *Genome Research*, 14, 1188–1190.
- Diallinas, G. and Martzoukou, O. (2019) Transporter membrane traffic and function: lessons from a mould. *The FEBS Journal*, 286, 4861–4875.
- Eddy, S.R. (1998) Profile hidden Markov models. *Bioinformatics*, 14, 755–763.
- Guldener, U., Heck, S., Fielder, T., Beinhauer, J. and Hegemann, J.H. (1996) A new efficient gene disruption cassette for repeated use in budding yeast. *Nucleic Acids Research*, 24, 2519–2524.
- Herzig, Y., Sharpe, H.J., Elbaz, Y., Munro, S. and Schuldiner, M. (2012) A systematic approach to pair secretory cargo receptors with their cargo suggests a mechanism for cargo selection by Erv14. *PLoS Biology*, 10, e1001329.
- Huang, Y., Niu, B., Gao, Y., Fu, L. and Li, W. (2010) CD-HIT Suite: a web server for clustering and comparing biological sequences. *Bioinformatics*, 26, 680–682.
- Käll, L., Krogh, A. and Sonnhammer, E.L.L. (2004) A combined transmembrane topology and signal peptide prediction method. *Journal of Molecular Biology*, 338, 1027–1036.
- Kamauchi, S., Mitsui, K., Ujike, S., Haga, M., Nakamura, N., Inoue, H., et al. (2002) Structurally and functionally conserved domains in the diverse hydrophilic carboxy-terminal halves of various yeast and fungal Na<sup>+</sup>/H<sup>+</sup> antiporters (Nha1p). *Journal of Biochemistry*, 131, 821–831.
- Katoh, K. and Standley, D.M. (2013) MAFFT multiple sequence alignment software version 7: improvements in performance and usability. *Molecular Biology and Evolution*, 30, 772–780.
- Kinclova-Zimmermannova, O. and Sychrova, H. (2006) Functional study of the Nha1p C-terminus: involvement in cell response to changes in external osmolarity. *Current Genetics*, 49, 229–236.
- Kinclova-Zimmermannova, O., Zavrel, M. and Sychrova, H. (2005) Identification of conserved prolyl residue important for transport activity and the substrate specificity range of yeast plasma membrane Na<sup>+</sup>/H<sup>+</sup> antiporters. *The Journal of Biological Chemistry*, 280, 30638–30647.
- Kinclova-Zimmermannova, O., Gaskova, D. and Sychrova, H. (2006) The Na<sup>+</sup>, K<sup>+</sup>/H<sup>+</sup>-antiporter Nha1 influences the plasma membrane potential of *Saccharomyces cerevisiae*. *FEMS Yeast Research*, 6, 792–800.
- Kinclova-Zimmermannova, O., Falson, P., Cmunt, D. and Sychrova, H. (2015) A hydrophobic filter confers the cation selectivity of *Zygosaccharomyces rouxii* plasma-membrane Na<sup>+</sup>/H<sup>+</sup> antiporter. *Journal of Molecular Biology*, 427, 1681–1694.
- Kinclova, O., Potier, S. and Sychrova, H. (2001a) The *Candida albicans* Na<sup>+</sup>/H<sup>+</sup> antiporter exports potassium and rubidium. *FEBS Letters*, 504, 11–15.
- Kinclova, O., Ramos, J., Potier, S. and Sychrova, H. (2001b) Functional study of the *Saccharomyces cerevisiae* Nha1p C-terminus. *Molecular Microbiology*, 40, 656–668.
- Krauke, Y. and Sychrova, H. (2008) Functional comparison of plasma-membrane Na<sup>+</sup>/H<sup>+</sup> antiporters from two pathogenic *Candida* species. *BMC Microbiology*, 8, 80.
- Krauke, Y. and Sychrova, H. (2011) Cnh1 Na<sup>+</sup>/H<sup>+</sup> antiporter and Ena1 Na<sup>+</sup>-ATPase play different roles in cation homeostasis and cell physiology of *Candida glabrata*. *FEMS Yeast Research*, 11, 29–41.
- Louie, R.J., Guo, J., Rodgers, J.W., White, R., Shah, N., Pagant, S., et al. (2012) A yeast phenomic model for the gene interaction network modulating CFTR-DeltaF508 protein biogenesis. *Genome Medicine*, 4, 103.
- Martzoukou, O., Karachaliou, M., Yalellis, V., Leung, J., Byrne, B., Amillis, S., et al. (2015) Oligomerization of the UapA purine transporter is critical for ER-exit, plasma membrane localization and turnover. *Journal of Molecular Biology*, 427, 2679–2696.
- Masrati, G., Dwivedi, M., Rimon, A., Gluck-Margolin, Y., Kessel, A., Ashkenazy, H., et al. (2018) Broad phylogenetic analysis of cation/proton antiporters reveals transport determinants. *Nature Communications*, 9, 4205.
- Mikosch, M. and Homann, U. (2009) How do ER export motifs work on ion channel trafficking? *Current Opinion in Plant Biology*, 12, 685–689.
- Mitsui, K., Yasui, H., Nakamura, N. and Kanazawa, H. (2005) Oligomerization of the *Saccharomyces cerevisiae* Na<sup>+</sup>/H<sup>+</sup> antiporter Nha1p: Implications for its antiporter activity. *Biochimica et Biophysica Acta*, 1720, 125–136.
- Nakanishi, H., Suda, Y. and Neiman, A.M. (2007) Erv14 family cargo receptors are necessary for ER exit during sporulation in *Saccharomyces cerevisiae*. *Journal of Cell Science*, 120, 908–916.
- Navarrete, C., Petrežselyova, S., Barreto, L., Martínez, J.L., Zahrádka, J., Ariño, J., et al. (2010) Lack of main K<sup>+</sup> uptake systems in *Saccharomyces cerevisiae* cells affects yeast performance in both potassium-sufficient and potassium-limiting conditions. *FEMS Yeast Research*, 10, 508–517.
- Norholm, A.B., Hendus-Altenburger, R., Bjerre, G., Kjaergaard, M., Pedersen, S.F. and Kragelund, B.B. (2011) The intracellular distal tail of the Na<sup>+</sup>/H<sup>+</sup> exchanger NHE1 is intrinsically disordered: implications for NHE1 trafficking. *Biochemistry*, 50, 3469–3480.
- Omasits, U., Ahrens, C.H., Muller, S. and Wollscheid, B. (2014) Protter: interactive protein feature visualization and integration with experimental proteomic data. *Bioinformatics*, 30, 884–886.
- Pagant, S., Wu, A., Edwards, S., Diehl, F. and Miller, E.A. (2015) Sec24 is a coincidence detector that simultaneously binds two signals to drive ER export. *Current Biology*, 25, 403–412.



- Papadaki, G.F., Amillis, S. and Diallinas, G. (2017) Substrate specificity of the FurE transporter is determined by cytoplasmic terminal domain interactions. *Genetics*, *207*, 1387–1400.
- Papadaki, G.F., Lambrinidis, G., Zamanos, A., Mikros, E. and Diallinas, G. (2019) Cytosolic N- and C-Termini of the *Aspergillus nidulans* FurE transporter contain distinct elements that regulate by long-range effects function and specificity. *Journal of Molecular Biology*, *431*, 3827–3844.
- Papouskova, K. and Sychrova, H. (2006) *Yarrowia lipolytica* possesses two plasma membrane alkali metal cation/H<sup>+</sup> antiporters with different functions in cell physiology. *FEBS Letters*, *580*, 1971–1976.
- Paulino, C., Wohlert, D., Kapotova, E., Yildiz, O. and Kuhlbrandt, W. (2014) Structure and transport mechanism of the sodium/proton antiporter MjNhaP1. *eLife*, *3*, e03583.
- Powers, J. and Barlowe, C. (1998) Transport of Axl2p depends on Erv14p, an ER-vesicle protein related to the *Drosophila cornichon* gene product. *The Journal of Cell Biology*, *142*, 1209–1222.
- Powers, J. and Barlowe, C. (2002) Erv14p directs a transmembrane secretory protein into COPII-coated transport vesicles. *Molecular Biology of the Cell*, *13*, 880–891.
- Pribylova, L., Papouskova, K. and Sychrova, H. (2008) The salt tolerant yeast *Zygosaccharomyces rouxii* possesses two plasma-membrane Na<sup>+</sup>/H<sup>+</sup>-antiporters (ZrNha1p and ZrSod2-22p) playing different roles in cation homeostasis and cell physiology. *Fungal Genetics and Biology*, *45*, 1439–1447.
- Pribylova, L., Papouskova, K., Zavrel, M., Souciet, J.L. and Sychrova, H. (2006) Exploration of yeast alkali metal cation/H<sup>+</sup> antiporters: sequence and structure comparison. *Folia Microbiologica*, *51*, 413–424.
- Prior, C., Potier, S., Souciet, J.L. and Sychrova, H. (1996) Characterization of the NHA1 gene encoding a Na<sup>+</sup>/H<sup>+</sup>-antiporter of the yeast *Saccharomyces cerevisiae*. *FEBS Letters*, *387*, 89–93.
- Proft, M. and Struhl, K. (2004) MAP kinase-mediated stress relief that precedes and regulates the timing of transcriptional induction. *Cell*, *118*, 351–361.
- Rosas-Santiago, P., Zimmermannova, O., Vera-Estrella, R., Sychrova, H. and Pantoja, O. (2016) Erv14 cargo receptor participates in yeast salt tolerance via its interaction with the plasma-membrane Nha1 cation/proton antiporter. *Biochimica et Biophysica Acta*, *1858*, 67–74.
- Rosas-Santiago, P., Lagunas-Gomez, D., Yanez-Dominguez, C., Vera-Estrella, R., Zimmermannova, O., Sychrova, H., et al. (2017) Plant and yeast cornichon possess a conserved acidic motif required for correct targeting of plasma membrane cargos. *Biochimica et Biophysica Acta*, *1864*, 1809–1818.
- Rosas-Santiago, P., Lagunas-Gomez, D., Barkla, B.J., Vera-Estrella, R., Lalonde, S., Jones, A., et al. (2015) Identification of rice cornichon as a possible cargo receptor for the Golgi-localized sodium transporter OsHKT1;3. *Journal of Experimental Botany*, *66*, 2733–2748.
- Roth, S., Neuman-Silberberg, F.S., Barcelo, G. and Schubach, T. (1995) cornichon and the EGF receptor signaling process are necessary for both anterior-posterior and dorsal-ventral pattern formation in *Drosophila*. *Cell*, *81*, 967–978.
- Sacristan, C., Manzano-Lopez, J., Reyes, A., Spang, A., Muniz, M. and Roncero, C. (2013) Oligomerization of the chitin synthase Chs3 is monitored at the Golgi and affects its endocytic recycling. *Molecular Microbiology*, *90*, 252–266.
- Sharpe, H.J., Stevens, T.J. and Munro, S. (2010) A comprehensive comparison of transmembrane domains reveals organelle-specific properties. *Cell*, *142*, 158–169.
- Schneider, T.D. and Stephens, R.M. (1990) Sequence logos: a new way to display consensus sequences. *Nucleic Acids Research*, *18*, 6097–6100.
- Schwenk, J., Harmel, N., Zolles, G., Bildl, W., Kulik, A., Heimrich, B., et al. (2009) Functional proteomics identify cornichon proteins as auxiliary subunits of AMPA receptors. *Science*, *323*, 1313–1319.
- Simon, E., Barcelo, A. and Arino, J. (2003) Mutagenesis analysis of the yeast Nha1 Na<sup>+</sup>/H<sup>+</sup> antiporter carboxy-terminal tail reveals residues required for function in cell cycle. *FEBS Letters*, *545*, 239–245.
- Simon, E., Clotet, J., Calero, F., Ramos, J. and Arino, J. (2001) A screening for high copy suppressors of the *sit4 hal3* synthetically lethal phenotype reveals a role for the yeast Nha1 antiporter in cell cycle regulation. *The Journal of Biological Chemistry*, *276*, 29740–29747.
- Smidova, A., Stankova, K., Petrvalska, O., Lazar, J., Sychrova, H., Obsil, T., et al. (2019) The activity of *Saccharomyces cerevisiae* Na<sup>+</sup>, K<sup>+</sup>/H<sup>+</sup> antiporter Nha1 is negatively regulated by 14-3-3 protein binding at serine 481. *Biochimica et Biophysica Acta*, *1866*, 118534.
- Springer, S., Malkus, P., Borchert, B., Wellbrock, U., Duden, R. and Schekman, R. (2014) Regulated oligomerization induces uptake of a membrane protein into COPII vesicles independent of its cytosolic tail. *Traffic*, *15*, 531–545.
- Thor, F., Gautschi, M., Geiger, R. and Helenius, A. (2009) Bulk flow revisited: transport of a soluble protein in the secretory pathway. *Traffic*, *10*, 1819–1830.
- Vacic, V., Oldfield, C.J., Mohan, A., Radivojac, P., Cortese, M.S., Uversky, V.N., et al. (2007) Characterization of molecular recognition features, MoRFs, and their binding partners. *Journal of Proteome Research*, *6*, 2351–2366.
- Velkova, K. and Sychrova, H. (2006) The *Debaryomyces hansenii* NHA1 gene encodes a plasma membrane alkali-metal-cation antiporter with broad substrate specificity. *Gene*, *369*, 27–34.
- Wallis, J.W., Chrebet, G., Brodsky, G., Rolfe, M. and Rothstein, R. (1989) A hyper-recombination mutation in *S. cerevisiae* identifies a novel eukaryotic topoisomerase. *Cell*, *58*, 409–419.
- Wudick, M.M., Portes, M.T., Michard, E., Rosas-Santiago, P., Lizzio, M.A., Nunes, C.O., et al. (2018) CORNICHON sorting and regulation of GLR channels underlie pollen tube Ca<sup>2+</sup> homeostasis. *Science*, *360*, 533–536.
- Zahradka, J. and Sychrova, H. (2012) Plasma-membrane hyperpolarization diminishes the cation efflux via Nha1 antiporter and Ena ATPase under potassium-limiting conditions. *FEMS Yeast Research*, *12*, 439–446.
- Zahradka, J., van Heusden, G.P. and Sychrova, H. (2012) Yeast 14-3-3 proteins participate in the regulation of cell cation homeostasis via interaction with Nha1 alkali-metal-cation/proton antiporter. *Biochimica et Biophysica Acta*, *1820*, 849–858.
- Zimmermannova, O., Felcmanova, K., Rosas-Santiago, P., Papouskova, K., Pantoja, O. and Sychrova, H. (2019) Erv14 cargo receptor participates in regulation of plasma-membrane potential, intracellular pH and potassium homeostasis via its interaction with K<sup>+</sup>-specific transporters Trk1 and Tok1. *Biochimica et Biophysica Acta*, *1866*, 1376–1388.

## SUPPORTING INFORMATION

Additional supporting information may be found online in the Supporting Information section.

**How to cite this article:** Papouskova K, Moravcova M, Masrati G, Ben-Tal N, Sychrova H, Zimmermannova O. C5 conserved region of hydrophilic C-terminal part of *Saccharomyces cerevisiae* Nha1 antiporter determines its requirement of Erv14 COPII cargo receptor for plasma-membrane targeting. *Mol Microbiol*. 2021;115:41–57. <https://doi.org/10.1111/mmi.14595>